

INSTITUTE FOR HIGH ENERGY PHYSICS

IHEP 93-106

V.B.Gorodnichev, V.A.Kachanov, V.Yu.Khodyrev, I.L.Kurchaninov,
V.V.Rykalin, V.L.Solovianov, M.N.Ukhanov

**STUDY OF POSITION RESOLUTION
AND ELECTRON-HADRON SEPARATION
OF ELECTROMAGNETIC CALORIMETER
WITH A SILICON STRUCTURE**

Submitted to *NIM*

Protvino 1993

VOL 27 № 09

Abstract

Gorodnichev V.B. et al. Study of Position Resolution and Electron-Hadron Separation of Electromagnetic Calorimeter: IHEP Preprint 93-106. – Protvino, 1993. – p. 12, figs. 10, tables 1, refs.: 8.

The maximum shower silicon strip detectors embedded in a module of sandwich-type electromagnetic calorimeter have been tested. The position resolution at different depths of the silicon structure has been measured. The results on electron-hadron separation obtained as a byproduct in this study are presented, and possibility of their improvement is discussed.

Аннотация

Городничев В.Б. и др. Изучение координатного разрешения и электрон-адронной сепарации электромагнитного калориметра с кремниевой стриповой плоскостью : Препринт ИФВЭ 93-106. – Протвино, 1993. – 12 с., 10 рис., 1 табл., библиогр.: 8.

Детектор максимума ливня, основанный на стриповой кремниевой плоскости, вставленной в модуль электромагнитного калориметра, был протестирован. Измерено координатное разрешение в зависимости от глубины залегания кремниевой плоскости. Была измерена электрон-адронная сепарация и обсуждена возможность её улучшения.

INTRODUCTION

We present the results on the study of silicon strip detectors installed inside the module of electromagnetic sandwich-type calorimeter (tungsten-scintillator) and used for improvement of its position resolution.

Usage of special detector for coordinate measurements inside an electromagnetic calorimeter decreases the number of channels and cost. Proportional gas chambers [1] and scintillating fibers [2] have already been used for this purpose. Silicon strip or pad detector seems to be very appropriate for a number of reasons. Silicon detector has no internal amplification so it is stable when fully depleted. There is no need for a gas system as for proportional chambers. It operates under relatively low working voltage. Silicon detector is more compact and reliable than proportional chambers. It is intrinsically very fast. The absence of sensitivity to magnetic field is another attractive feature of this type of detectors. The technology of such detectors has been developing very intensively in the past years and detectors of various types have been produced.

Such calorimeter can be useful at future accelerators *LHC*[3], *SSC*, *UNK*, especially in heavy ion collision, where the number of secondary particles can exceed several thousands. For this reason the separation of γ and electrons with the distance between them less than one centimeter and efficient rejection of electron from hadron is necessary.

1. DETECTORS

The module design is illustrated on Fig 1. The sandwich has 18 units of radiation length X_0 and is made of $1.5 \times 40 \times 40$ mm tungsten and $4 \times 40 \times 40$ mm scintillator tiles. We used a wavelength shifter to collect light on a photomultiplier, which provided the signal of total energy deposition in the

module. From our point of view this choice of absorption material and module construction provides small value of Moliere radius needed for good coordinate measurements. Additional usage of the position sensitive detector installed inside the module allows one to have relatively raw transverse segmentation of the total absorption calorimeter.

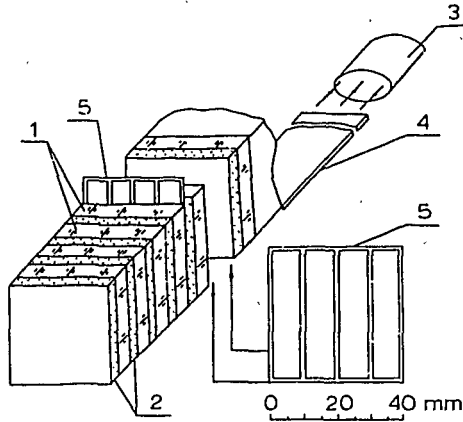


Figure 1. View of the module: 1 - 4 mm of scintillator; 2 - 1.5 mm of tungsten; 3 - photo-multiplier; 4 - wavelength shifter; 5-5' - silicon plates.

The silicon detector design and technology of fabrication procedure were described in [4]. The basic characteristics of the silicon detectors are given in Table 1. To reduce the time needed for measurements we used two of them.

Table 1. Properties of the silicon detectors (for one strip)

Mechanical thickness	300 μm
Depletion depth	280 μm
Resistance of silicon	$2 \div 4 \text{ K}\Omega \cdot \text{cm}$
Operating voltage	100 V
Maximum leakage current at full depletion	200 nA
Capacitance at full depletion	130 pF

2. PREAMPLIFIER CHOICE

We used a hybrid preamplifier [5] with the following characteristics: the *ENC* value was 4300 electrons (R.M.S.) at the detector capacitance about 120 pF. The signal width at 0.1 amplitude was about 80 ns. A shaping amplifier is not necessary in this scheme which lowers the cost and simplifies the design of big multichannel systems. The signal amplitude range was in accordance with *ADC* linearity region. We did not optimize the signal to noise ratio and time characteristics of the front-end electronics, because it was not the main purpose of our investigation and had small impact on the results.

3. EXPERIMENTAL CONDITIONS AND MONTE-CARLO MODEL

The measurements were carried out on 26 GeV electron and 39 GeV π^- beams of beam line 14 at IHEP, Protvino. Signals from scintillation counters *S1* – *S3*, *A0* (Fig. 2) formed the trigger strobe, which activated registration of particle position in the microstrip hodoscope *MSD* and digitization of signals from the silicon strips and *PM*. Fast amplification of signals from the silicon detectors allowed us to use the same *ADCs* [6] as for *PM*. The length of the strobe for both types of signals was equal to 100 ns.

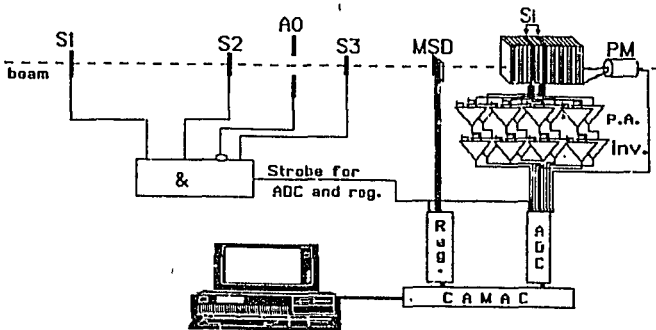


Figure 2. Schematic view of the test set-up: *S1* – *S3*, *A0* – scintillation counters; *MSD* – microstrip hodoscope; *PM* – photomultiplier; *S_i* – the silicon structures; *P.A.* – preamplifiers; *Inv.* – inverters.

The data of hodoscope registers and the *ADCs* were read by IBM/PC compatible computer for on-line analysis and archiving. On-line software allowed visualization of the amplitude spectra from *ADCs* and imposed the cut on the multiplicity of hits in the *MSD*. Selection of events with only one hit in the *MSD* let us suppress the effect of electrons showering in the matter of the beam path.

All results of our measurements were compared with Monte-Carlo simulations based on GEANT V.3.15 package. The program model reproduced all the essential features of the experimental set-up except electronic noise, so the simulation results can be considered as a border in improvement of the signal / noise ratio for the electronics.

4. DATA ANALYSIS AND RESULTS OF THE MEASUREMENTS

At the first step of data analysis we evaluated calibration coefficients c_i which set accordance of *ADC* counts A_i with ionization E_i in a strip i of the silicon detector:

$$E_i = c_i A_i.$$

The silicon structure was placed in front of the module and each strip was exposed to electron beam. Assuming the amplitude spectra of signal A_i^{cal} (Fig. 3) to be produced by minimum ionizing particles (*MIP*), we defined calibration coefficients as

$$c_i = \frac{1}{\langle A_i^{cal} \rangle},$$

where $\langle A_i^{cal} \rangle$ are mean values of *MIP* spectra. This choice of normalization let us measure the ionization produced by the shower inside the sandwich in "*MIP*" units.

The following measurements were carried out on 26 *GeV* electron beam with the depth silicon detectors varying from 2 to 16 layers of tungsten that was about 1 to 7 units of radiation length X_0 . A cut in low amplitudes from *PM*, used in data analysis, eliminated muon and hadron components of the beam from further consideration. Trying to minimize the effect of shower leakage, we exposed on the beam only central part of the module surface about 1 *cm* wide.

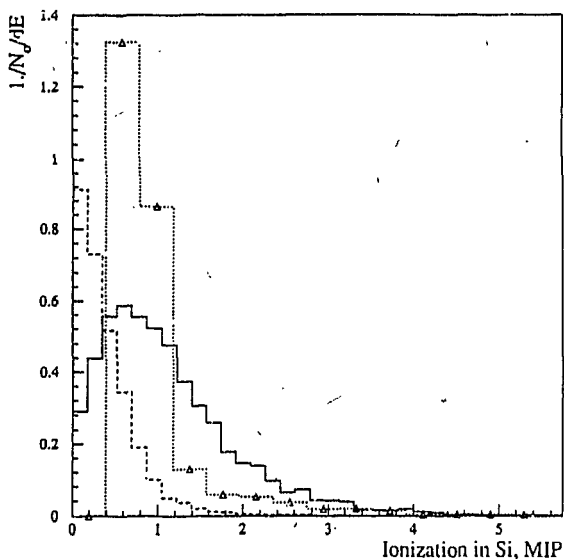


Figure 3. Amplitude spectra from a silicon strip placed in front of the sandwich: solid line - experimental spectrum produced by electrons; dashed line - electronic noise (no particle coming through); dotted line and Δ - GEANT Monte Carlo in the same scale.

Further analysis was made for each of the silicon plates separately, because of significant correlations of their signals. A typical distribution of ionization $E = \sum_{i=1}^4 E_i$ for the structure placed after 11 layers of the sandwich is shown on Fig. 4. The Gaussian function fits the spectrum fairly well. We observed that non-uniformity of mean energy deposition $\langle E \rangle$ along the exposed surface, which might be connected with calibration precision, variation of depleted thickness within silicon strip and shower leakage, did not exceed 10%. Fig. 5 shows another important feature of the shower from 26 GeV electron - its longitudinal development. A good agreement of experimental results with GEANT simulation assured us in linearity of the silicon detector and electronics.

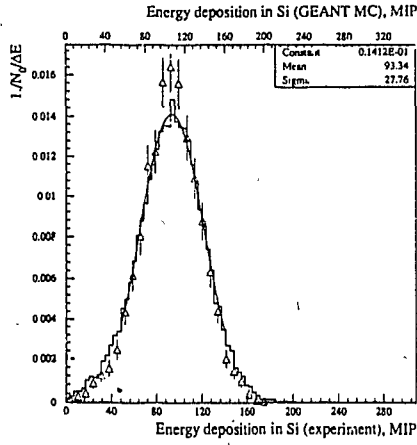


Figure 4. Ionization spectrum in the silicon plate placed after 11 layers of the sandwich (4.7 units of X_0): Solid line – experiment along with Gaussian fit; Δ – Monte Carlo simulation.

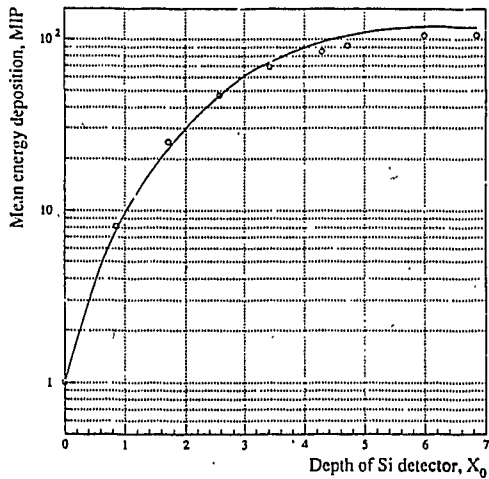


Figure 5. Mean ionization in the silicon plate plotted against its depth in the sandwich: \circ – experiment; solid line – Monte Carlo simulation.

4.1. Position Resolution of the Silicon Structure

A full study of position resolution of the calorimeter was carried out when the silicon detectors were placed after 11, 14, and 16 layers of the module that lies just about the measured maximum of showers produced by 26 GeV electrons. We chose this region as a reasonable compromise between demands for the minimal transverse size of the shower and maximal part of the shower energy, detected by the silicon structure.

For each of those depths we measured the dependence of the shower center of gravity

$$X_{Si} = \frac{\sum_{i=1}^4 X_i E_i}{\sum_{i=1}^4 E_i}$$

on true position X_{real} of electron impact. Fig. 6 shows this dependence, computed with GEANT, for the structure placed after 11 module layers, along with polynomial approximation. $X_{real} = 0$ corresponds to the center of the module; the error bars represent the spread of X_{Si} for a point like beam. The experimental curve was the same within its precision. One can see that some leakage of the shower energy results in the bias of X_{Si} at the strip center, at $|X_{real}| = 5$ mm. However, the effect of leakage on position resolution was not essential.

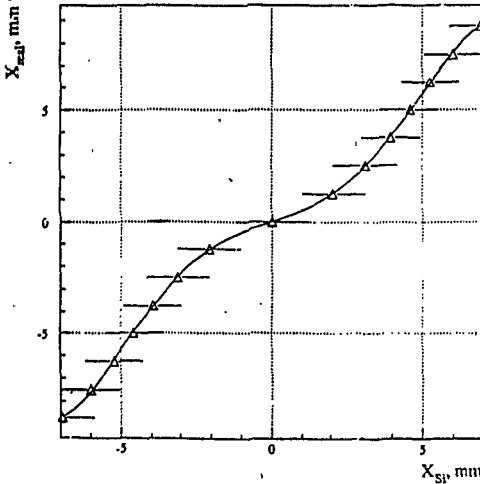


Figure 6. The shower center of gravity X_{Si} , computed with GEANT, plotted against real impact position X_{real} on the calorimeter surface. The silicon detector is placed after 11 modules layers. The solid curve represents polynomial approximation.

The polynomial approximations were used to evaluate unbiased position of the impact point X_{cat} . Fig. 7 represents the shadow of 0.6 mm wide strip of the *MSD*, as it is seen by the silicon detector near the border of strips (a) and the center of a strip (b). GEANT gave practically the same results, with an exception for the tails of the distributions, connected with limited efficiency of *MSD*.

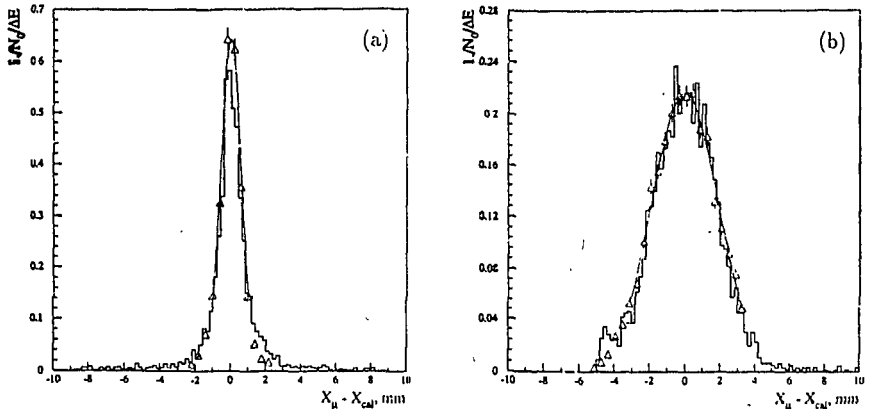


Figure 7. Position resolution of the silicon detector after 11 layers of the sandwich. Solid histogram – experiment; Δ and curve – Monte Carlo. (a) – for electron impact point between strips; (b) – for the impact point at the strip center.

As one can see on Fig. 8, at the strip boundary the resolution increases almost linearly with the depth of the position sensitive plate. This is connected with an increase of the shower width as it develops in the sandwich. Our conclusion is that a smaller strip size will not improve the resolution at the fixed depth of the detector.

The behaviour of resolution in the strip center is mainly determined by its dimensions, since a major part of the shower energy contained by a single channel of the detector. The consequence is the improvement of the resolution as the silicon plate is getting deeper in the sandwich and the shower is becoming wider. Evidently, a smaller strip size will improve the coordinate accuracy in this case.

The comparison of experimental resolution with Monte-Carlo computed on gave another important result. We came to a conclusion that electronic noise had no essential effect on the measurements with the silicon detector placed near the shower maximum. Intrinsic shower fluctuations put the main limitation on the accuracy.

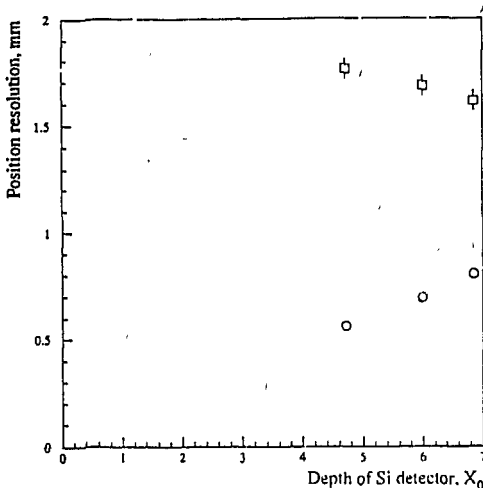


Figure 8. The measured dependance of position resolution of the silicon detector on its depth in the sandwich: o - for electron impact point between strips; □ - for the impact point at the strip center.

4.2. Electron-Hadron Separation

The module was tested on beams of pions at 39 GeV and electrons at 26 GeV to estimate the electron-hadron separation possibility. The rejection coefficient R is defined as probability to take a hadron for electron for given electron detection probability. In our case a pion is taken for electron if its energy deposition in the calorimeter exceeds given threshold. The threshold defines efficiency for an electron to be detected. There is a possibility to improve the separation by a silicon plate inserted inside the sandwich and simultaneously using the information about total energy deposition.

The information about summary energy deposition from the silicon detector only gives $R = (16 \pm 0.4) \cdot 10^{-3}$ with 90% electron efficiency. Choice of events with additional condition (signal from the photomultiplier must be over threshold too) gives $R = (6.5 \pm 0.2) \cdot 10^{-3}$ for 90% efficiency for electrons.

To check our test results the Monte-Carlo simulation was carried out. R calculated by the last method is: $R = (6.9 \pm 0.9) \cdot 10^{-3}$. The distributions calculated by Monte-Carlo for energy deposition of pions and electrons in the silicon detector and total deposition in the calorimeter module are presented on Fig. 9 and 10, respectively.

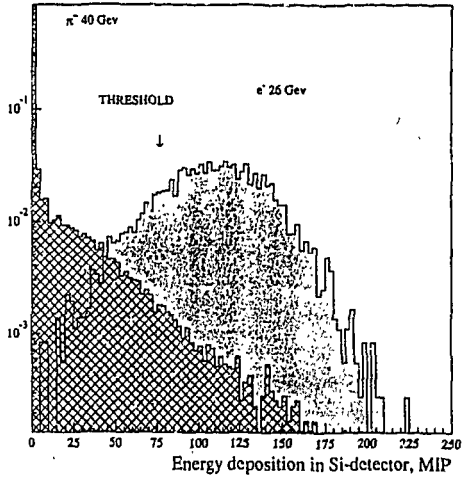


Figure 9. Energy deposition in Si detector for pions and electrons calculated by Monte Carlo.

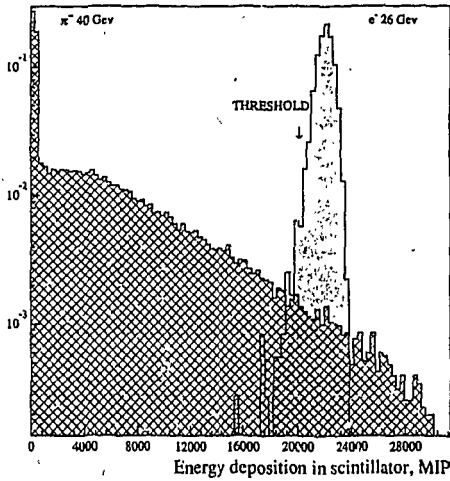


Figure 10. Energy deposition in scintillator for pions and electrons calculated by Monte Carlo.

The results of our investigations of the electron-hadron separation is in agreement with the data published in [7,8].

CONCLUSION

The silicon detector being inserted in the tungsten-scintillator sampling calorimeter was tested on hadron and electron beams with energy 39 GeV and 26 GeV, respectively.

The dependence of the coordinate resolution on the plate depth in the module was measured on electron beam and compared with Monte Carlo simulation. Position resolution better than 1 mm near the shower maximum is feasible. The electron-hadron separation improved by information from the silicon plate was measured. The observed value was close to $6 \cdot 10^{-3}$ and appeared to be compatible with Monte Carlo simulations.

A good agreement of our measurements with simulations, where electronic noise was ignored, has drawn us to the conclusion about correct choice of the preamplifier. This type of front-end electronics with fast response and wide dynamic range seems to be very suitable for shower detectors with embedded silicon pads as coordinate sensitive detector.

ACKNOWLEDGEMENTS

We gratefully acknowledge the help of our colleagues of NEPTUN collaboration whose cooperation made these tests possible. We are grateful to our technical staff, in particular, S.Alexeev.

References

- [1] Balka L. et al. // NIM. 1988. V. A267 p.272.
- [2] Chuiko B. et al. – IHEP Preprint 92-104, Protvino, 1992.
- [3] Proceedings of the ECFA-CERN Workshop on the Large Hadron Collider, CERN 90-10, 1990, vol.2.
- [4] Barkov I.P. et al.//Pribory i Tekhnika Eksperimenta. 1992. №5. P. 56-62.
- [5] Golovin V.M. et al.//Pribory i Tekhnika Eksperimenta. 1991. №1. P. 132-133.
- [6] Alde D. et al. // NIM. 1990. V. A240. P. 343.

[7] UA1 Collaboration CERN. Performance of Uranium/Tetramethyl-Pentane Calorimeter Backed by an *Fe/Sci* CERN-PPE/90-171.

[8] The ZEUS Detector. Status Report 1987. P. 5-73 – 5-75.

Received August, 18, 1993

Городзичев В.Б. и др.

Изучение координатного разрешения и электрон-адронной сепарации электромагнитного калориметра с кремниевой стриповой плоскостью.

Оригинал-макет подготовлен с помощью системы $\text{\AA}\text{T}_{\text{E}}\text{X}$.

Редактор А.А. Антипова. Технический редактор Н.В. Орлова.

Корректор Е.И. Горина.

Подписано к печати 24.08.1993 г.

Формат 60 × 90/16.

Офсетная печать. Печ.л. 0,94. Уч.-изд л. 0,75. Тираж 260. Заказ 903.

Индекс 3649.

Институт физики высоких энергий, 142284, Протвино Московской обл.

